A DAMAGE TOLERANT BIO-INSPIRED INTEGRATED COMPOSITE STIFFENER VIA AFP

A.D. Whitehouse[1]*, Y. Yang[1], V. Médeau[1], L. Mencattelli[1], E. Greenhalgh[1], and S.T. Pinho[1]

[1] Department of Aeronautics, Imperial College, London, UK
* Corresponding author (adw15@ic.ac.uk)

Keywords: Bio-inspired, Damage Tolerant, Composite Structures, Stiffener, Automated Fibre Placement

ABSTRACT

Stiffened composite panels are vulnerable to rapid debonding of the stiffeners, which has resulted in the development of conservative certification requirements. In this work, inspired by the branch-trunk attachment of trees, an embedded composite stiffener is developed in the pursuit of damage tolerant panels. Improved damage tolerance can pave the way for more ambitious certification requirements, which will allow for more efficient aircraft designs to be realised. Automated Fibre Placement (AFP) is increasingly utilised by industry; in this work, stiffened panels are developed which can be preformed in a single AFP process. This paper presents the results of this manufacturing endeavour, the use of a foam core and curved hat stiffener geometry is validated as an AFP manufacturing route for composite stiffened panels. Preliminary experimental results, using a notched compression configuration, of the bio-inspired embedded concept are presented. Initial stable crack growth and prevention of debonding ahead of the notch tip are demonstrated. Finally, a numerical parametric study is presented for a modified notched compression specimen design to be used in an upcoming comprehensive experimental study of the concept.

1 INTRODUCTION

Stiffened composite panels are essential in aerospace as they are a mass-effective solution to provide structural stiffness and stability to the underlying panels [1]. However, the threat of traditional bonded stiffeners suffering rapid brittle fracture, known as ‘unzipping’, has contributed to the development of conservative certification requirements for commercial airliners [2]. If stiffened structures can be developed which exhibit superior damage tolerance, less conservative certification requirements can hence be developed. This would allow for significant reductions in aircraft weight, resulting in reduced fuel consumption and costs. This envisaged weight reduction is imperative to making aircraft with alternative fuels (such as hydrogen) viable, and hence to achieving NetZero in aviation.

Longitudinal hat stiffeners (also known as omega stiffeners) are common in both the Boeing 787 and the Airbus A350XWB [3]. A more damage-tolerant design would hence allow for a reduction in the weight of such type of aircraft. More generally, the development of less conservative certification requirements, enabled by a more damage-tolerant design, may widen the scope of feasible aircraft structures. In turn, this may enable more efficient aircraft designs, such as aircraft with high-aspect ratio wings and Blended Wing Body (BWB) aircraft [4], which is key for the utilisation of alternative fuels and is critical for attaining NetZero aviation [5].

In the pursuit of sustainability, sustainable and efficient manufacture needs to be considered simultaneously with the design. Automated Fibre Placement (AFP) is being increasingly adopted by industry over manual layup as it offers improved material efficiency, increased production rates, and improved preform quality and consistency [6–8]. Whilst composite skins are usually manufactured via AFP, the stiffeners are typically manufactured separately, then co-cured or bonded in a secondary process. A damage-tolerant stiffened panel design, which would simultaneously allow the full panel to be manufactured in-situ via AFP, would be highly desirable for future aircraft.

In this work, we propose an original bio-inspired embedded composite stiffened panel, manufactured via AFP, to provide improved damage tolerance relative to a traditional co-cured stiffener design. In this paper, we firstly propose the bio-inspired damage-tolerant embedded concept, and then explain the modified stiffened panel design which enables AFP manufacture. We then present our experimental methods, results and discussion of preliminary notched compression tests, and a numerical parametric study to guide upcoming experimental work. Finally, a summary of the most important conclusions is provided.

2 CONCEPT FOR A DAMAGE TOLERANT STIFFENED PANEL VIA AFP

2.1 Bio-inspired embedded stiffener concept

In this work, we propose an embedded composite stiffener to achieve improved damage tolerance which is inspired by the embedding of the branch into the centre of the trunk at tree-branch attachments (Figure 1). Trees are subject to significant structural and dynamic loads due to the force of their own weight and the varied dynamic force of the wind. Despite the composition of wood including brittle constituents, such as lignin and hemi-cellulose, tree-branch attachments have evolved to exhibit remarkable strength and damage tolerance.

Burns et al. [2] conducted X-ray tomography of branch attachments, shown in Figure 1, and found three key contributing design features: integration of the branch by embedding it into the centre of the trunk; orientation of fibrils along the direction of the principal stress; and variable fibril packing density to achieve iso-strain conditions.

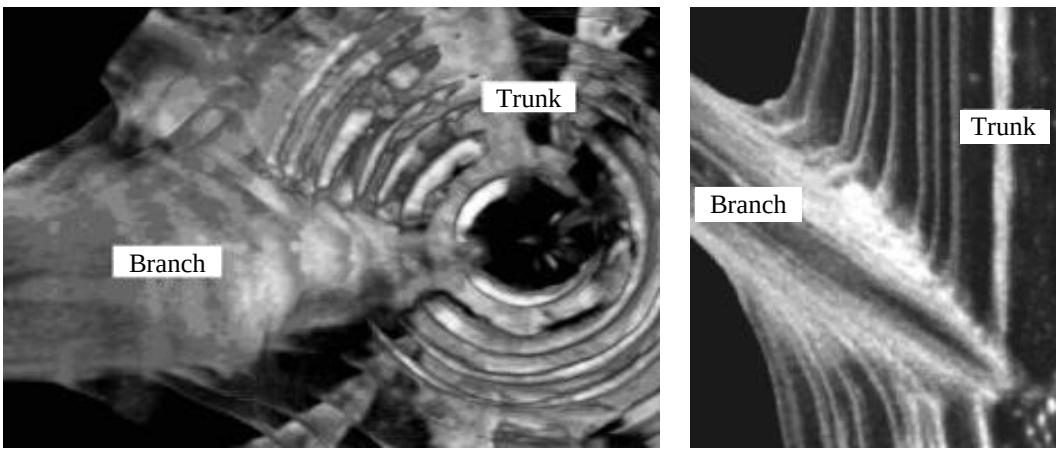

Figure 1: CT scans of a *Pinus radiata* tree, showing the integration of the branch into the trunk [2].

Inspired by this, Burns et al. developed composite T-joints which combined these bio-mimetic features synergistically [9], resulting in increases to both failure initiation load, and normalised strain energy to failure.

The schematics in Figure 2 show our proposal for an embedded hat stiffener design, inspired by the embedding of the branch into the centre of the trunk at tree-branch attachments, compared to a baseline traditional co-cured design. In a traditional design, such as that depicted in Figure 2 (b), the plies which constitute the stiffener all terminate at the end of the flange, and the attaching interface between the stiffener flange and the panel skin, which is critical for load transfer, is vulnerable to debonding.

In our proposed bio-inspired embedded design, as shown in Figure 2 (c), continuous plies from the global skin (skin remote from the stiffener), continue into both branches of the stiffened section, embedding the stiffener within the panel. This prevents debonding of the stiffened section and the

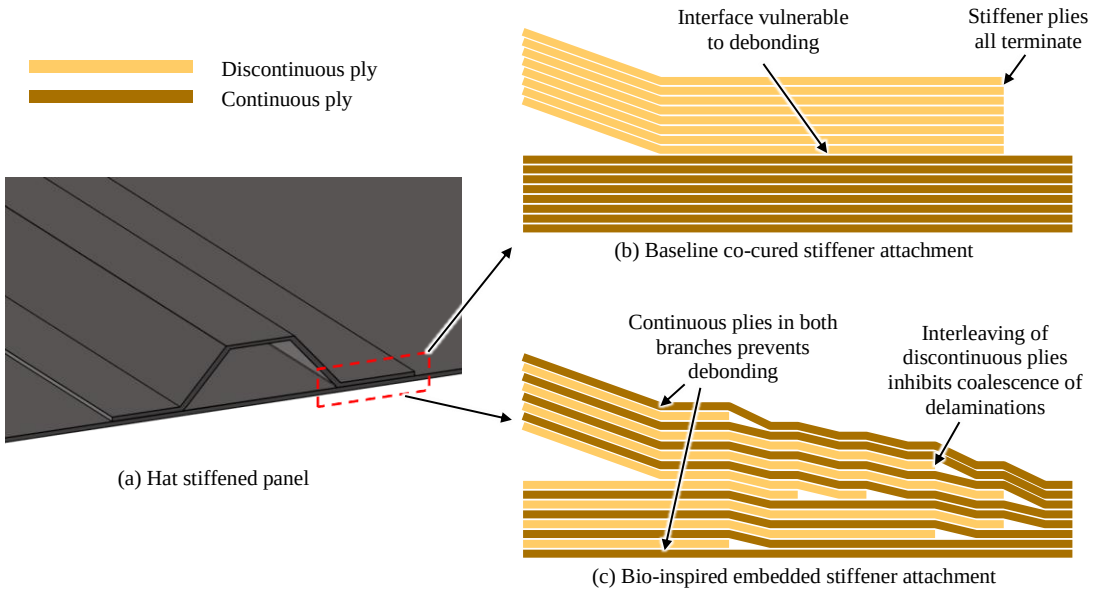

Figure 2: Ply-drop schematics of a typical stiffener relative to the proposed bio-inspired design.

associated sudden loss of stability. Additional plies are added in the stiffened region to form the desired layups in each branch; these discontinuous plies are interleaved between the continuous plies to improve damage diffusion by inhibiting the coalescence of delaminations.

Figure 3 shows the layup orientation strategies used for the baseline and bio-inspired designs in the current work. The baseline specimen skin and stiffener laminates have simple quasi-isotropic layups: $[45/0/-45/90]_s$. In the bio-inspired design, the global skin used this same layup, whilst the laminate sections in the stiffened region have quasi-isotropic layups with a different stacking sequence: $[45/90/0/-45]_s$, to enable the interleaved design using the same set of plies.

In the embedded design, the plies are dropped according to the literature guidelines for ply drops in tapered laminates [10], with plies containing fibres parallel to the terminating edge dropped closest to the thick section, and plies with fibres perpendicular to the terminating edge extending closest to the thin section.

2.2 AFP compatible stiffener design

A concept which is damage tolerant, but which also manufacturable via AFP, is highly desirable for the aerospace industry. To manufacture the stiffener with AFP, a suitable mould choice is required, and a manufacturable cross-section is required for the stiffener. The baseline stiffener configuration developed in this work is shown in Figure 4.

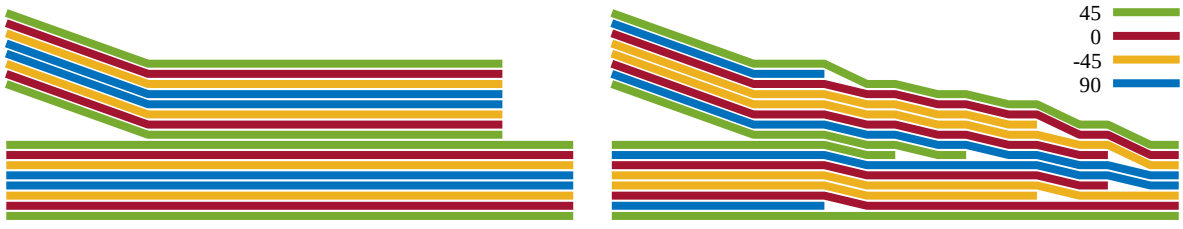

Figure 3: Layup orientation strategies in the two designs.

Figure 4: Section view of a hat stiffener configuration designed to be compatible with AFP.

A high-performance structural foam was chosen to act as both the mould for manufacture, and as a structural core in the final part. The manufacturing process is simplified relative to a mould which is required to be removed from the cured part, and low-density structural foams provide both improved stiffener stability and impact damage tolerance for a relatively low mass penalty when used as structural cores.

We modified the section geometry from that of a traditional hat-stiffener so that it is optimised for AFP manufacture: in particular, it contains larger relative radii of curvature on both the concave and convex corners. The larger curvature successfully prevents kinking of fibres which are laid across the corners, and additionally prevents fibre bridging in the concave region during AFP manufacture. The concave curvature was increased by a greater extent to ensure suitable compaction of axial and +/-45° tows.

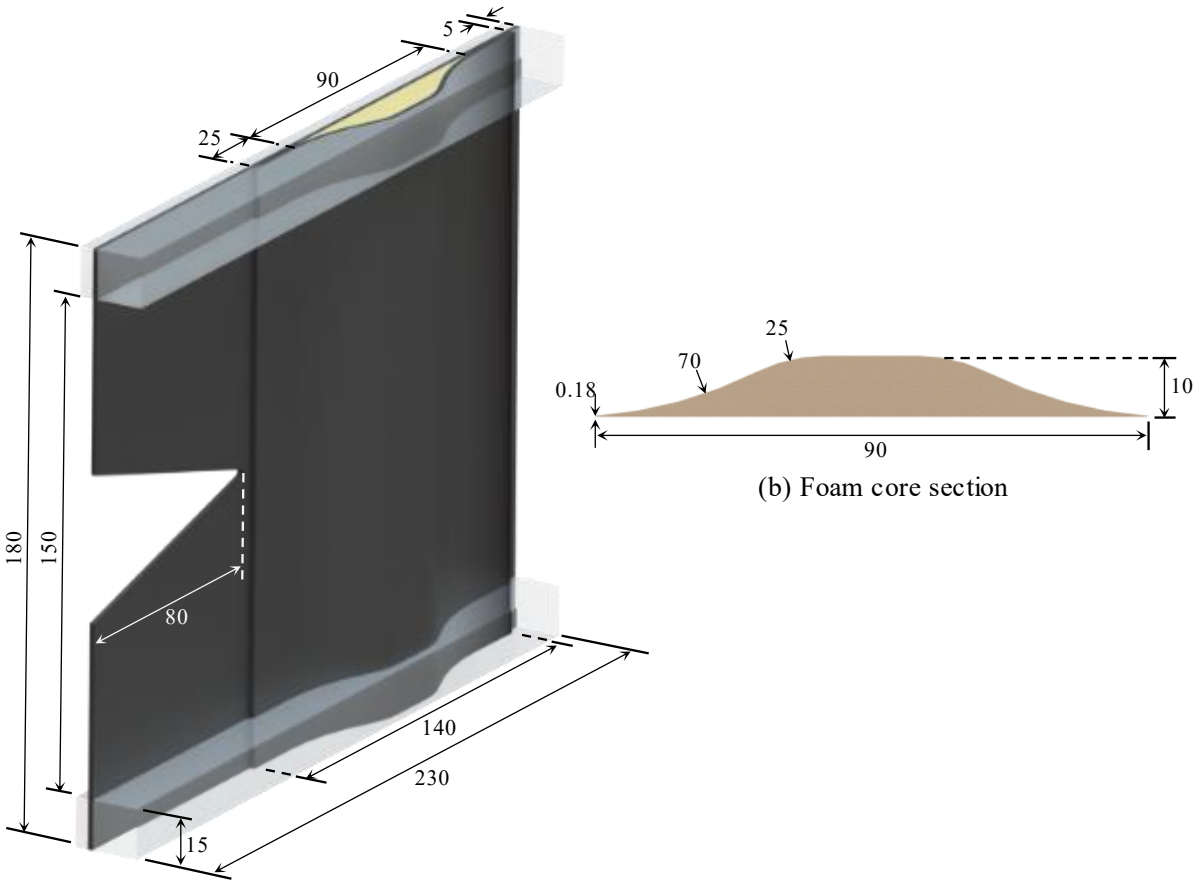

(a) Prototype notched compression specimen

(b) Foam core section

Figure 5: Specimen geometry following finetuning of the geometry during the feasibility study. All dimensions are in millimetres.

3 FEASIBILITY STUDY

3.1 Prototype specimen

To assess the feasibility of manufacturing and testing our bio-inspired specimen as described in section 2, we started by developing a suitable prototype specimen (Figure 5). This prototype specimen allowed for:

- developing the AFP manufacturing procedure, fine-tuning the manufacturing parameters for the particular slit-ply pre-preg used, and also finetuning the geometry of the specimen to optimise the deposition quality; and
- developing the test setup, to ensure the best possible monitoring of the key aspects of the test.

Stiffeners provide stability to skins, and a most challenging case for a stiffener is when a translaminar crack (eventually due to and in combination with buckling) propagates towards the stiffener. For this reason, our prototype specimen, used for material and test setup development, contains a notch to ensure that a translaminar crack propagates towards the flange of the stiffener.

The notch tip is 5 mm from the beginning of the stiffened region. The initial crack length is 80 mm to reduce the load of fracture propagation relative to other undesirable failure modes. Potted ends provide built-in boundary conditions to help prevent global buckling before fracture propagation. The stiffener is 140 mm wide including an embedded region, or flanges, spanning 25 mm at either side of the foam core. The panels are composed of M21E/IMA carbon fibre from Hexcel [11] and ROHACELL® 71 HERO structural polymethacrylimide (PMI) foam from Evonik [12]. GlassCast50 epoxy casting resin [13] was used for the end potting. Material properties are provided in Table 1.

M21E/IMA laminate [11,14,15]							
E	146 GPa	$G_{12} = G_{13}$	5.2 GPa	$\nu_{12} = \nu_{13}$	0.34	t_{ply}	0.184 mm
$E_{22} = E_{33}$	9.3 GPa	G_{23}	3.1 GPa	ν_{23}	0.5	$G_{\text{IC}}^{\text{lam}}$	80 kJm^{-2}
Hero71 foam [12]							
E_{c}	48 MPa			ν	0.3		
GlassCast50 casting resin [13]							
E	3 GPa			ν	0.3		

Table 1: Properties of the materials used in the study.

3.2 Manufacturing development

We utilised a Carbon Axis XCell AFP machine [16] for the preform layup. We generated a CAD model for all of the desired ply shapes, then generated toolpaths and machine code using the associated XLay software package [17]. We used simulations of toolpaths to verify the generated program as depicted in Figure 6a.

Manufacture of the pre-form is shown in Figure 6b. First, we deposited the flat plies; the initial layer was deposited on Mylar® A film to achieve sufficient tack for successful deposition. We then positioned the foam, pre-machined to shape on a CNC router and cleaned with compressed air, on the part using pin and bolt holes in the ends of the foam to locate and secure it to the turntable during the layup procedure. We subsequently deposited the 3D plies on top of the flat preform and foam. We utilised the angle-cut capability of the AFP machine to achieve a straight edge at ply-drops/the flange edge for all ply orientations. We carried out various iterations of manufacturing, ending up with the precise stiffener shape shown in Figure 5 and corresponding AFP manufacturing parameters, which are ideally suited for

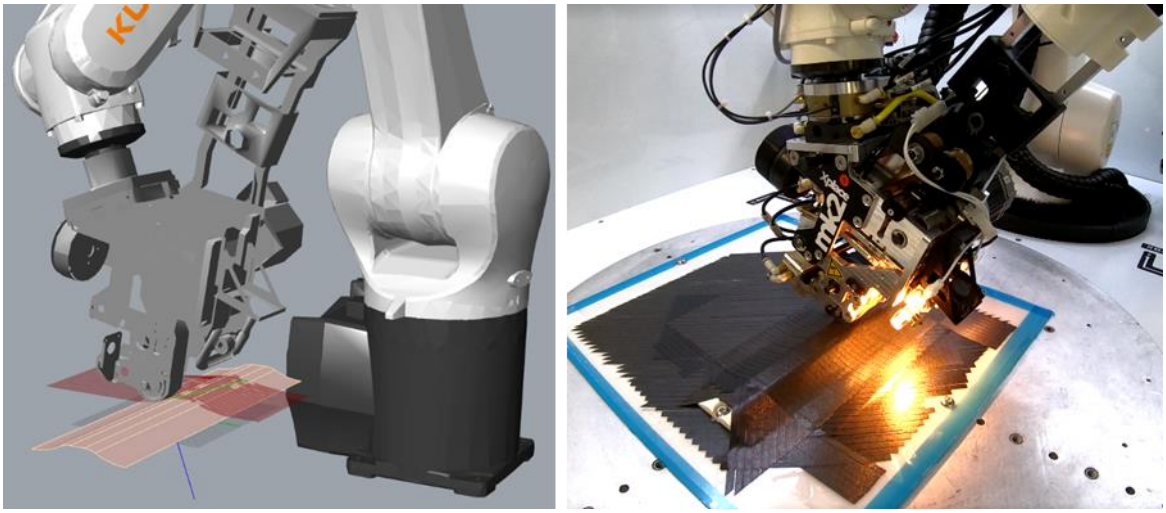

(a) XLay CAD – simulating toolpaths (b) XCell hardware – preform manufacture

Figure 6: 3D preform manufacture utilising Carbon Axis AFP. Timelapse of manufacture of the bio-inspired panel available online at: youtu.be/h2dmyUdVw78

the use of the AFP setup used in this study.

We cured the successfully-manufactured preforms in an autoclave as per the foam-compatible cure cycle in the pre-preg manufacturer's data sheet [11]. Following curing, we cut the specimens from the cured panels using a water-jet cutter. We cut the notch during this process and a crack tip radius of 0.8 mm was achieved.

We potted the specimen ends to a depth of 15 mm in GlassCast® 50 clear epoxy casting resin [13] to provide built-in boundary conditions. To ensure correct alignment of the specimen during potting, we clamped them against angle plates with parallels utilised as spacers to ensure suitable positioning of the specimen in the potting mould. Once the resin had cured, we removed the specimens from the moulds and ground the ends flat to provide a suitable face for the compression test.

3.3 Test setup development

The final setup developed using the prototype specimens is shown in Figure 7. We conducted the tests using an Instron 5985 universal testing machine with a 250 kN load cell. We used a die-set fixture to apply the compressive forces to the specimen which ensures, via linear bearings, that only axial loads are transferred to the testing machine. We clamped Acoustic Emission (AE) sensors to each specimen to detect damage events. We painted the specimens white with a black speckle pattern to enable the use of Digital Image Correlation (DIC). We positioned cameras to record the test section of the specimen for DIC, and positioned a camera looking down the notch. The specimen was centred and lightly squeezed, then square steel bars were positioned against the potting faces, and clamped to the die-set, to conservatively provide additional support to the built-in condition. The compression test was conducted at a loading rate of 0.5 mm/min.

4 RESULTS & DISCUSSION

4.1 AFP Compatible Manufacturing

We successfully achieved manufacture of high quality baseline and bio-inspired stiffened composite panels via AFP (Figure 8), with cross-section microscopy shown in Figure 9. The baseline, despite being co-cured, is visibly composed of two regions, with the edge of the stiffener clearly visible. In contrast,

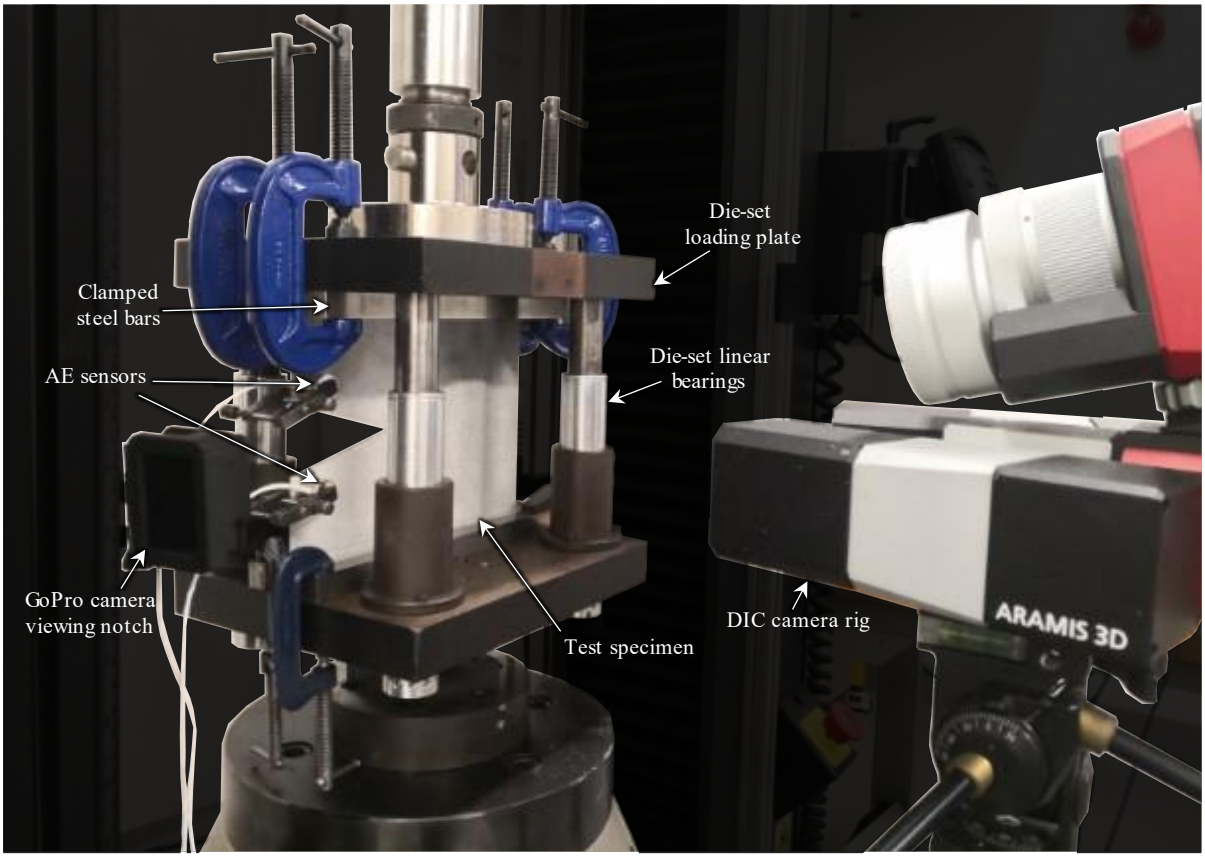

Figure 7: Experimental notched compression test set-up.

(a) Baseline specimen

(b) Bio-inspired specimen

Figure 8: Stiffened panel test specimens following water-jet cutting.

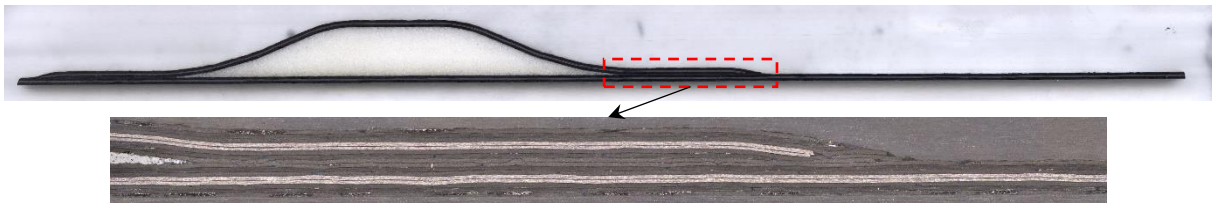

(a) Baseline specimen

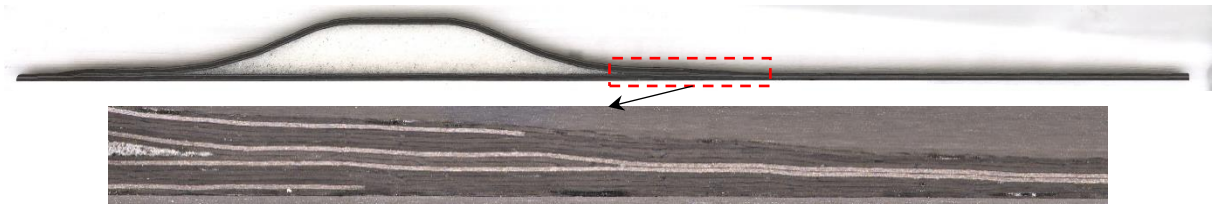

(b) Bio-inspired specimen

Figure 9: Section views, with the interface of skin and stiffener magnified.

the bio-inspired specimen gives a smooth transition away from the stiffened region and visibly has the appearance of a single integrated part. The bio-inspired embedding of the stiffener branch is seen in Figure 9b to have been achieved as per the design presented in Section 2.1, with the ply drops achieving an overall smooth tapering from the thick end to thin end. C-scans reveal no significant defects in either panel, and the cross-section microscopy reveals no significant voids.

4.2 Test setup development

Our test setup, including various cameras, DIC and AE sensors, was able to capture all the intended information during the tests, some of which is shown in Figure 10 and Figure 11. Furthermore, the prototype specimens generated qualitative data which provides evidence (Figure 10 & Figure 11) supporting that the bio-inspired design should provide a more damage tolerant structure if applied in composite stiffened panels, such as in aircraft fuselage or wing-box sections.

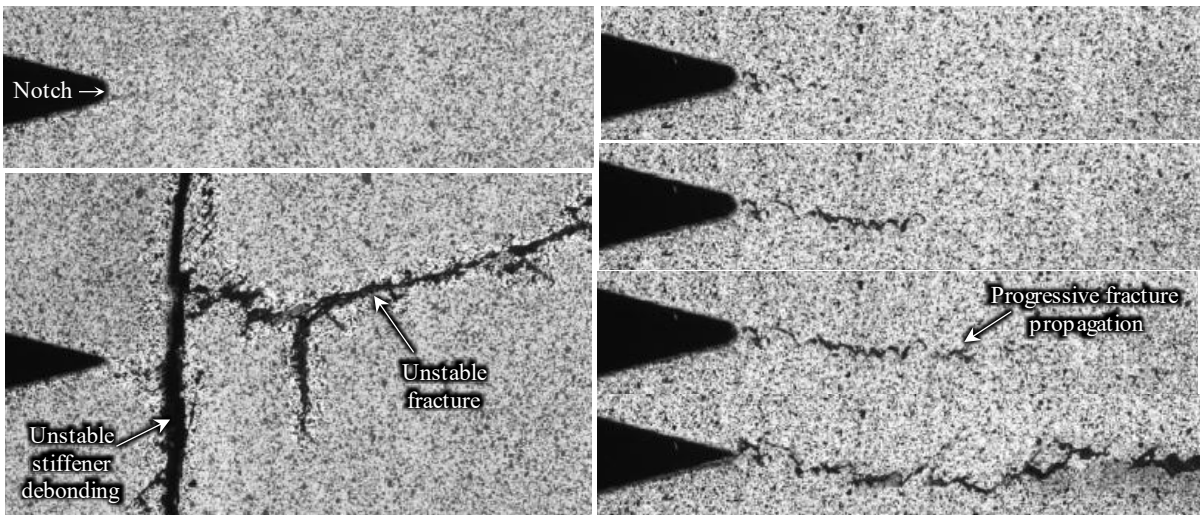

(a) Baseline: unstable failure (b) Bio-inspired: progressive failure

Figure 10: The vertically aligned images chronologically show each identifiable stage of crack progression.

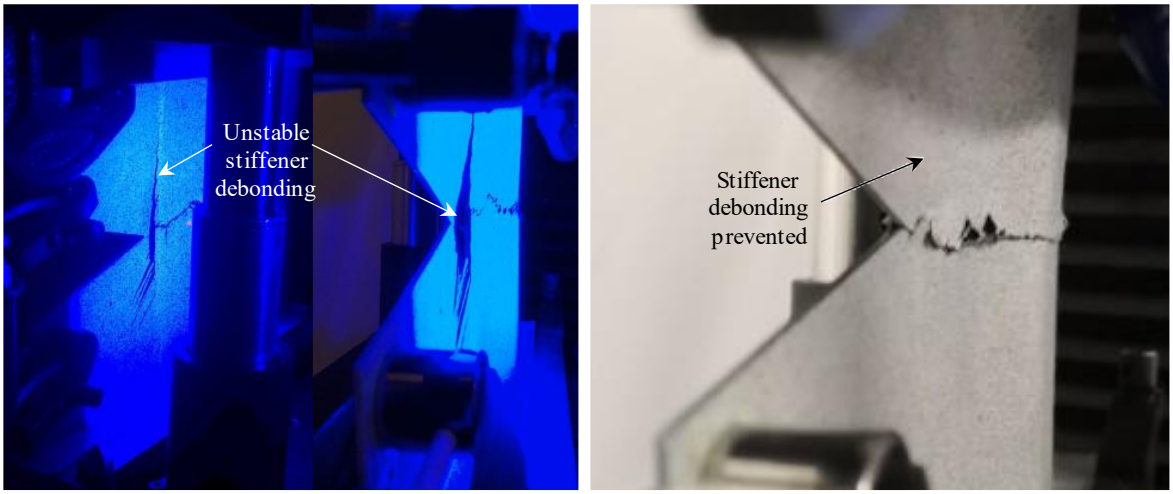

(a) Baseline - viewed from two angles (b) Bio-inspired

Figure 11: Damage at the notch tip and stiffener edge in each specimen.

In the baseline specimen, we observed minimal fracture propagation before ultimate failure resulted in propagation of the fracture and significant stiffener debonding. Figure 10a shows the crack tip immediately before and after failure in the baseline specimen, whilst Figure 11a shows the significant debonding of the stiffener after failure.

In the bio-inspired specimen, we observed stable fracture propagation in the embedded region prior to final failure, as shown in Figure 10b. The main failure was propagation of the fracture, and no visible separation of the embedded region near the notch was observed, as shown in Figure 11b.

5 NUMERICAL PARAMETRIC STUDY FOR FINAL SPECIMEN DESIGN

Following the successful AFP manufacturing and testing development (as well as broad concept validation as seen by the stable failure in Figure 10), we created a specimen design for an extensive experimental study that would test the concept in the most industrially relevant load case. In traditional stiffened panels, the stiffener stabilises the skin. Load is transferred from the skin to the stiffener at the interface, and if debonding occurs the stiffener can no longer support the skin which subsequently takes the full load. This accelerates buckling and propagation of any local fractures. We hence set about designing a specimen to replicate this load case. To achieve this, load must be transferred to the stiffener at the 'interface'. Therefore, the stiffener must not be directly loaded; as a result, compressive loading and potting will be directly applied only to the skin in the notched region (Figure 12), somewhat similarly to the configuration of a compact compression test.

We developed a numerical model in ABAQUS [18] to verify this specimen design, and any required amendments. We modelled the laminate with shell elements with reduced integration (S4R), with tie constraints at the relevant surfaces to the foam which we modelled with solid elements with reduced integration (C3D8R). The potting was also modelled with solid elements with reduced integration, and an 'embedded region' constraint to the specimen geometry.

We completed both a buckling analysis and J-integral analysis, and the resulting ratio of fracture initiation load and buckling load compared. All displacements on the faces which would be directly compressed were prevented, other than the axial displacement on the top face, where a displacement of 1 mm (J-integral analysis), or a load of 1 N (buckling analysis), was applied depending on the analysis type. The meshing strategy is shown in Figure 12. We used a structured global mesh, with element side lengths of 2 mm, and a refined structured region with element side lengths of 0.2 mm was used at the

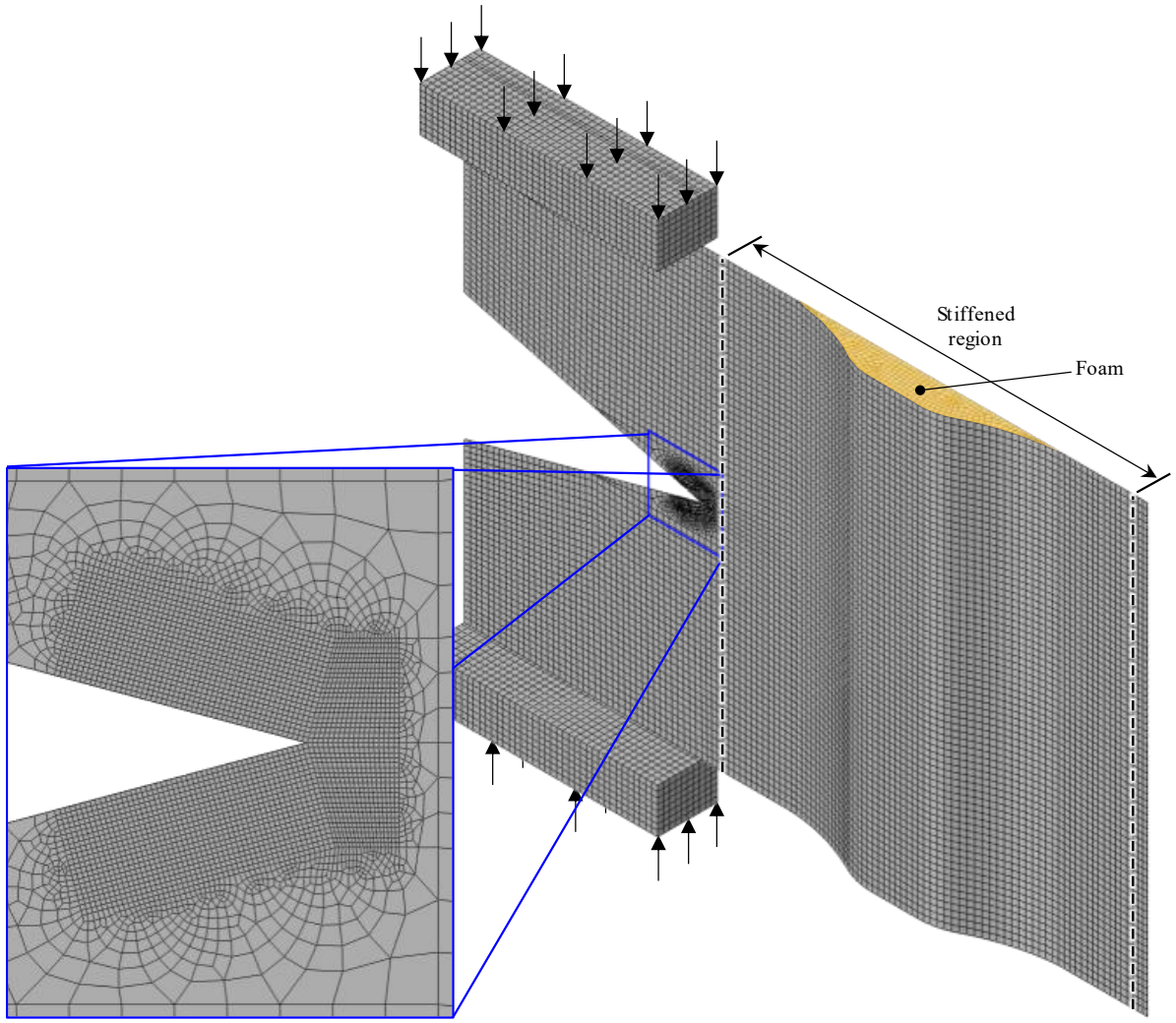

Figure 12: The mesh refinement strategy used in the numerical model.

crack tip, with a free region transitioning between the two. Suitable mesh convergence studies were carried out.

The anticipated fracture load from the J-integral analysis is given as

$$P_{fracture} = P_{FE}\sqrt{\frac{G_{IC}^{lam}}{J_{FE}}} \tag{2}$$

where J_{FE} is the J-integral of the numerical model, $G_{\mathrm{IC}}^{\mathrm{lam}}$ is the mode-I translaminar fracture toughness of the laminate, and P_{FE} is the load in the FE model.

Simulation results for the initial configuration revealed that global out of plane buckling, shown in Figure 13a, would occur at 7.45 kN prior to propagation of fracture at 15.4 kN (assuming no buckling had occurred). To obtain a specimen design which would achieve fracture propagation following local buckling of the skin, but prior to global buckling, we developed a python script to parameterise the model (available online dx.doi.org/10.17632/gbf7tjvngk.1). The effect of various parameters were investigated, including: the loading length, notch length, and specimen length. Various boundary conditions were also investigated, varying the region potted at the top and bottom edge, and the use of skin stability tabs in the loading region.

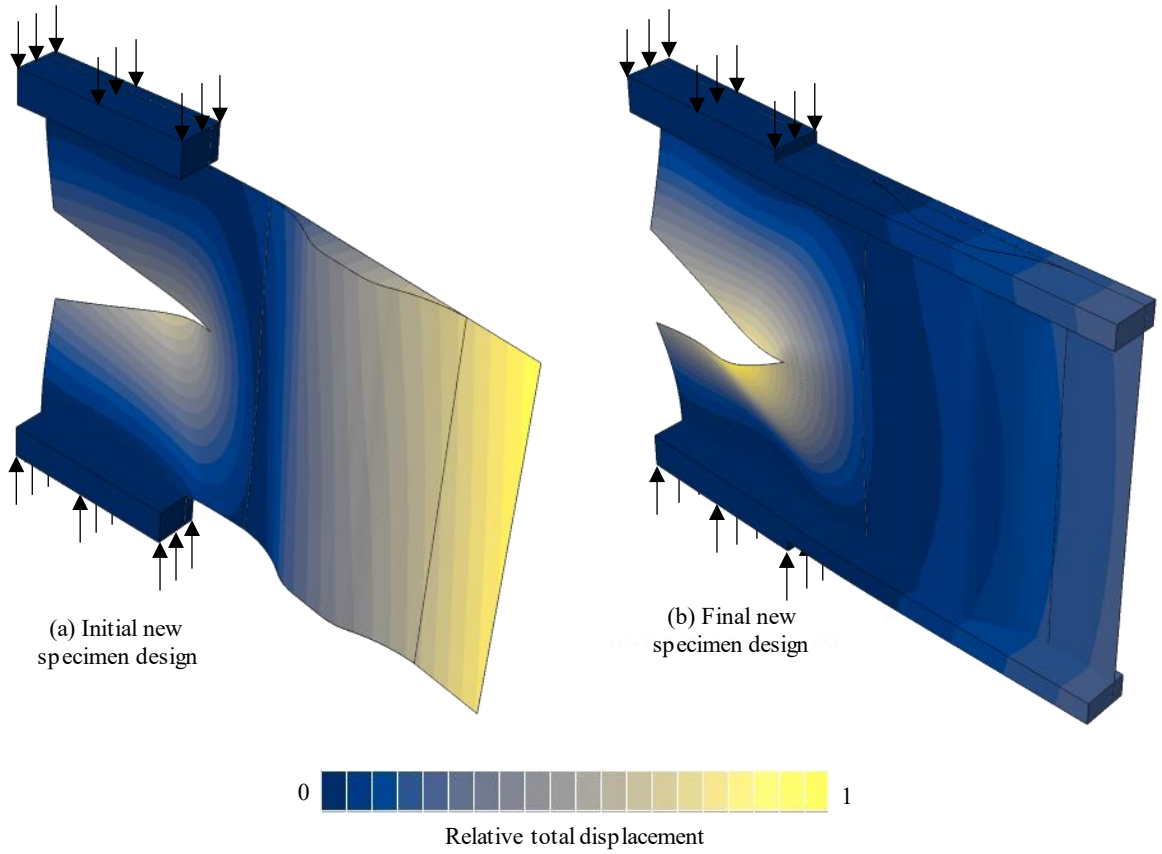

Figure 13: The first buckling mode of the new specimen designs.

A specimen design with loading only along the notched skin, and with the potting extended across the entire top and bottom edge, successfully prevented global out of plane buckling. Local skin buckling would occur, as shown in Figure 13b, at 11.9 kN, whilst fracture propagation would occur at a slightly higher load of 18.5 kN not accounting for the buckling. Therefore, this specimen configuration should replicate the desired industrially-relevant failure mechanism of crack propagation driven by local skin instability. We have now begun manufacturing specimens with this configuration, to provide an extensive experimental analysis of the bio-inspired stiffener concept which we will show at the conference.

6 CONCLUSIONS

In this paper, we identified the importance of developing damage-tolerant stiffened composite panels, and the desirability of an AFP manufacturing route. We designed a bio-inspired damage-tolerant stiffened panel utilising a foam core, and successfully manufactured these panels with AFP. Notched compression tests revealed that the bio-inspired concept was successful in achieving stable crack growth and suppressing debonding of the stiffener. A parametric study with numerical models has been conducted to design a notched compression specimen which reflects the importance of the skin-stiffener attachment in industrial applications, and which tests the concept in the most challenging load case. Manufacture of these specimens for an extensive experimental study is underway and will be presented at the conference.

ACKNOWLEDGEMENTS

The authors would like to gratefully acknowledge the funding for this work from EPSRC DTP 2020-2021 grant reference no. EP/T51780X/1, and the funding from Innovate UK under the UKRI

FANDANGO project No. 113232. For the purpose of open access, the author has applied a Creative Commons Attribution (CC BY) licence to any Author Accepted Manuscript version arising.

REFERENCES

[1] Ji R, Zhao L, Wang K, Liu F, Gong Y, Zhang J. Effects of debonding defects on the postbuckling and failure behaviors of composite stiffened panel under uniaxial compression. Compos Struct 2021;256:113121. https://doi.org/10.1016/J.COMPSTRUCT.2020.113121.

[2] Burns LA, Mouritz AP, Pook D, Feih S. Bio-inspired design of aerospace composite joints for improved damage tolerance. Compos Struct 2012;94:995–1004. https://doi.org/10.1016/J.COMPSTRUCT.2011.11.005.

[3] Hiken A. The Evolution of the Composite Fuselage: A Manufacturing Perspective. Aerosp Eng 2019. https://doi.org/10.5772/INTECHOPEN.82353.

[4] Brown M, Vos R. Conceptual design and evaluation of blended-wing-body aircraft. AIAA Aerosp Sci Meet 2018 2018. https://doi.org/10.2514/6.2018-0522.

[5] Bergero C, Gosnell G, Gielen D, Kang S, Bazilian M, Davis SJ. Pathways to net-zero emissions from aviation. Nat Sustain 2023 2023:1–11. https://doi.org/10.1038/s41893-022-01046-9.

[6] Lukaszewicz DHJA, Ward C, Potter KD. The engineering aspects of automated prepreg layup: History, present and future. Compos Part B Eng 2012;43:997–1009. https://doi.org/10.1016/J.COMPOSITESB.2011.12.003.

[7] Brasington A, Sacco C, Halbritter J, Wehbe R, Harik R. Automated fiber placement: A review of history, current technologies, and future paths forward. Compos Part C Open Access 2021;6:100182. https://doi.org/10.1016/J.JCOMC.2021.100182.

[8] Zhang L, Wang X, Pei J, Zhou Y. Review of automated fibre placement and its prospects for advanced composites. J Mater Sci 2020;55:7121–55. https://doi.org/10.1007/s10853-019-04090-7.

[9] Burns LA, Mouritz AP, Pook D, Feih S. Strength improvement to composite T-joints under bending through bio-inspired design. Compos Part A Appl Sci Manuf 2012;43:1971–80. https://doi.org/10.1016/J.COMPOSITESA.2012.06.017.

[10] Allegri G, Kawashita L, Backhouse R, Wisnom M, Hallett S. On the optimization of tapered composite laminates in preliminary structural design. Proc. ICCM17 Conf. EICC, Edinburgh, UK; 27th–31st July, 2009.

[11] HexPly ® M21 2020.

[12] Evonik Operations GmbH. Technical Information ROHACELL® HERO 2022.

[13] Easy Composites Ltd. GlassCast® 50 Clear Epoxy Casting Resin - Technical Datasheet n.d.

[14] Llobet J, Maimí P, Essa Y, Martin de la Escalera F. Progressive matrix cracking in carbon/epoxy cross-ply laminates under static and fatigue loading. Int J Fatigue 2019;119:330–7. https://doi.org/10.1016/J.IJFATIGUE.2018.10.008.

[15] Pinho S, Vyas G, Robinson P. Material and structural response of polymer-matrix fibre-reinforced composites: Part B. J Compos Mater 2013;47:679–96. https://doi.org/10.1177/0021998313476523.

[16] Hardware – Carbon Axis | Automated Fibre Placement n.d. https://www.carbon-axis.com/hardware/ (accessed January 4, 2023).

[17] Software – Carbon Axis | Automated Fibre Placement n.d. https://www.carbon-axis.com/software/ (accessed April 23, 2023).

[18] Dassault Systemes. Abaqus Standard 2021.